Tellus (1990), *42B*, 149–161

Atmospheric trace gases and global climate: a seasonal model study

By WEI-CHYUNG WANG*, GYULA MOLNAR, MALCOLM K. W. KO, STEVEN GOLDENBERG and NIEN DAK SZE, *Atmospheric and Environmental Research, Inc., 840 Memorial Drive, Cambridge, MA 02139, USA*

(Manuscript received 14 June 1988; in final form 2 January 1989)

ABSTRACT

Observations have shown that concentrations of atmospheric trace gases CO_2, CFCs, CH_4 and N_2O have been increasing and the trend of increases will most likely continue. Increases of these radiatively and chemically important trace gases may have implications for global climate both directly by modifying the earth's radiation budget and indirectly by changing atmospheric O_3 distribution. Here, we use atmospheric models with seasonal cycles to study the changes in latitudinal and vertical distributions of atmospheric O_3 and temperature caused by increases of trace gases in the next few decades. It is found that increases of CFCs, CH_4, and N_2O may augment the surface warming expected from CO_2 increases. Using projected trends of CO_2, N_2O, CH_4 and CFCs, our calculations showed that the annual mean and global mean surface temperature could warm by as much as 2.5°C with larger warming at high latitudes by the middle of the next century. The calculations also suggest that the warming in the lower stratosphere and upper troposphere is much larger than that at the surface, especially during the summertime. Large stratosphere cooling is calculated with maximum cooling of ~12°C around 45 km, where O_3 depletion caused by increases of trace gases contributes substantially to the total cooling. However, the effects of O_3 changes on the temperatures below 40 km appear to be small because of the small changes calculated in the O_3 distribution.

1. Introduction

Atmospheric trace gas concentrations of carbon dioxide (CO_2), nitrous oxide (N_2O), methane (CH_4) and chlorofluorocarbons (CFCs) are observed to be increasing due to natural and anthropogenic activities. Apart from the well-documented upward trends observed for CO_2 (cf. DOE, 1985a) and CFCs (Cunnold et al., 1986), recent atmospheric measurements indicate that the concentrations of N_2O and CH_4 may also have increased in the past decade or perhaps longer (cf. WMO, 1986). There is additional support for the CH_4 trend from recent analyses of ground-based solar infrared spectra recorded in 1951 (Rinsland et al., 1985). Ice core samples also indicate lower concentrations for N_2O and CH_4 in the preindustrial era (Pearman et al., 1986).

Current estimates of future CO_2 increases are that the present level of CO_2 (~340 ppmv) will double some time in the next century (DOE, 1985a). Atmospheric measurements have shown an increase of 1% per year in the surface concentration of CH_4 since 1977 (cf. Blake and Rowland, 1988; Khalil and Rasmussen, 1986). However, it is unclear whether the observed increase is due to enhanced emission associated with changes in the biosphere or to changes in tropospheric hydroxyl radical (OH). The trend for N_2O is estimated to be between 0.2 and 0.3% per year between 1976 and 1980. Projections for the future are uncertain because of a lack of detailed information on the N_2O budget. Furthermore, a recent study by Khalil and Rasmussen (1989) suggests that changes in the earth's ecosystem during climate change may

* Atmospheric Sciences Research Center, State University of New York at Albany, Albany, New York, NY 12205, USA.

induce feedbacks on the global cycles of CH_4 and N_2O.

Similar to CO_2, increases in burdens of other atmospheric trace gases can cause greenhouse warming, a direct effect associated with the strong infrared absorption bands of these gases (see Wang et al., 1986). In addition, these trace gases are also chemically important; their increases may perturb the concentrations of ozone (O_3) and water vapor (H_2O) which may indirectly affect the climate (cf. DOE, 1985b; WMO, 1986).

Both N_2O and CFCs are associated with atmospheric removal of O_3 through catalytic processes involving chlorine and nitrogen cycles (WMO, 1986). However, the chlorine and nitrogen cycles are strongly coupled in the sense that increasing NO_x ($NO + NO_2$) in the stratosphere would dilute the impact of Cl on O_3. For instance, reactions of ClO with NO and NO_2 tend to suppress the concentrations of ClO (and thereby its effect on O_3) as NO_x increases.

Increasing CH_4 and CO_2, on the other hand, tends to increase O_3. Stratospheric temperatures are expected to be lower as CO_2 increases. A cooler stratosphere would reduce the efficiency of many catalytic O_3 removal cycles. Methane can affect O_3 in a number of ways. First, oxidation of CH_4, initiated by $CH_4 + OH \rightarrow CH_3 + H_2O$ is an important source of tropospheric O_3. Second, the reaction of CH_4 with Cl represents a major sink for active Cl and may therefore indirectly increase O_3 by reducing the impact of stratospheric Cl. Thirdly, oxidation of CH_4 is a source of stratospheric H_2O. Increasing H_2O (due to CH_4 increase) can increase stratospheric OH which enhances the efficiency of the chlorine cycle, but suppresses the nitrogen cycle.

Study of the direct greenhouse effect of the trace gases has been based on the use of one-dimensional (1-D) models, especially the radiative-convective models. The results suggest that the combined effects of the increases of CH_4, N_2O, and CFCs could warm the surface temperature comparable to that due to CO_2 increases. In recent years, these models have also been coupled with 1-D photochemical-transport models to study the trace gases climate-chemistry interactions (see Wang et al., 1986, and Ramanathan, et al., 1987 for a review). These studies indicate that the stratospheric cooling caused by CFCs-induced stratospheric O_3 depletion may also be comparable in magnitude to that caused by CO_2 increases and that the perturbation to atmospheric O_3 may have implications on tropospheric climate.

Recently, Wang and Molnar (1985) have used a mean annual, coupled low and high latitude radiative-dynamical model to study the direct greenhouse effect due to increases of trace gases. The results suggest that it is important to consider the latitudinal variations of the climate feedback processes such as humidity and vertical dynamical heat transport in the study of greenhouse effects. For example, observations indicate that the cumulus convection process dominates the temperature lapse rate in the low latitudes whereas baroclinic instability is more important in mid to high latitudes. As shown in Wang and Molnar (1985), incorporation of these latitudinally-dependent processes into the models would calculate a substantially smaller surface warming effect due to increases of trace gases than that calculated from the 1-D models. However, the combined effect of the increases of trace gases is still large and can substantially augment the CO_2 warming effect.

Both observational data and general circulation model (GCM) simulation indicate that the strength of the interactions between the radiative, vertical, and meridional dynamic heat fluxes is nonlinear and depends strongly on the seasons (cf. Stone, 1984; Hansen et al., 1984; Washington and Meehl, 1984). Wetherald and Manabe (1981) have compared the response of the seasonal model to the quadrupling of CO_2 with the corresponding response of the mean annual model. It is found that the response of the annual mean surface air temperature of the seasonal model is significantly less than the corresponding response of the mean annual model. The smaller sensitivity of the seasonal model is attributed to a smaller ice/snow albedo feedback because of the absence of strongly reflective snow cover during the summer when the solar insolation has a near maximum intensity. Consequently, the seasonal cycle needs to be included in the model to study the climatic effects due to increases of trace gases. Furthermore, our confidence in using the model for assessment of climatic effects of increasing trace gas concentration would be greatly enhanced if the model is

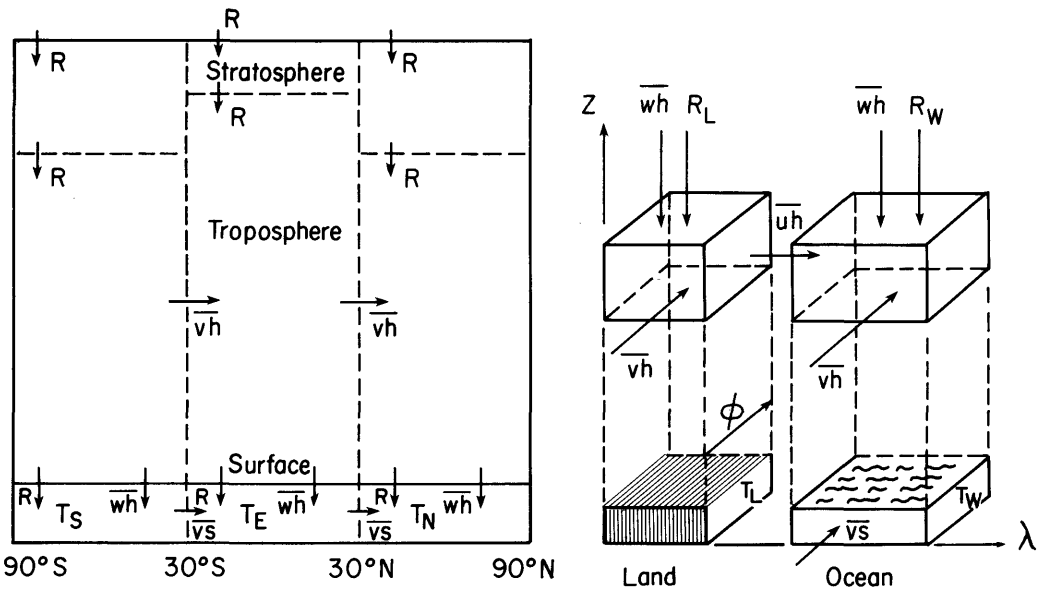

Fig. 1. Schematic illustration of the heat balance components of the global and seasonal radiative-dynamical climate model with three latitudinal zones and land/ocean sectors within each latitude zone. The coordinates of ϕ, λ, and z are latitude, longitude and altitude, respectively. Definition of the energy terms is given in Section 2.1.

capable of simulating the seasonal variations of the present climate, which constitutes an important part of model validation.

Here, we use seasonal atmospheric models to study the greenhouse effect of increases of trace gases and their associated O_3 changes. For the latter, previous studies using 2-D models concentrated more on the interpretation of the O_3 response and stratospheric temperature changes than the changes in surface temperature (Haigh and Pyle, 1982; Haigh, 1984; Eckman et al., 1987). To perform this study, we have used the latitudinal and vertical distributions of trace gases and O_3 calculated from the seasonal photochemical-transport model (Ko et al., 1985a, b) as inputs to the seasonal climate model. In this so-called "open-loop" study, the changes in trace gas distributions are calculated using the same set of prescribed values for temperatures and transport circulation in both the present-day atmosphere and perturbed atmospheres. Therefore, the changes in temperature and transport circulation associated with the change in radiative balance of the atmosphere are not taken into account for the trace gas calculations.

The seasonal model calculations cover the period 1960–2060 and use the observations of trace gas concentrations for 1960–1985 while scenarios are assumed for future growth. Note however that in the time-dependent calculations, the ocean heat capacity was not explicitly considered. Below, we briefly describe the atmospheric models in Section 2 and the model results are presented in Section 3.

2. Atmospheric models

2.1. Climate model

The climate model simulates the seasonal, latitudinal and vertical distribution of atmospheric temperature through energy balance. The model, shown in Fig. 1, is an extension of the annual model (Wang et al., 1984; Wang and Molnar, 1985; Gutowski et al., 1985) and includes three latitudinal zones representing the tropical latitudes (30°S–30°N), southern hemispheric extratropical latitudes (30°S–90°S), the southern zone and northern hemispheric extratropical latitudes (30°N–90°N), the northern zone. The atmosphere is divided into 8 layers in the stratosphere and 10 layers in the troposphere. Because of the large difference in thermal inertia between land and oceans, which is important in simulating the

seasonal cycle, both land and ocean sectors are included within each latitude zone.

The climate model computes the seasonal temperature from the heat balance for the atmosphere,

$$\frac{\partial}{\partial t}(c_p T + Lq) = \frac{-1}{r\cos\phi}\left[\frac{\partial}{\partial\lambda}(\overline{uh}) + \frac{\partial}{\partial\phi}(\overline{vh}\cos\phi)\right] - \frac{\partial}{\partial p}(\overline{wh}) - g\frac{\partial R}{\partial p}, \quad (1)$$

and for the subsurface (ocean/land) layer of depth Δz_s,

$$\frac{\partial}{\partial t}(c_s T) = \frac{-1}{r\cos\phi}\left[\frac{\partial}{\partial\lambda}(\overline{us}) + \frac{\partial}{\partial\phi}(\overline{vs}\cos\phi)\right] + \frac{1}{\rho_s g\,\Delta z_s}(\overline{w_0 h_0} + gR_0). \quad (2)$$

Here t is time, ϕ latitude, λ longitude, and p pressure; u, v and w are the eastward, northward and vertical velocities in pressure coordinates; r is the earth's radius, T temperature, q specific humidity, R the net downward radiative flux, ρ density, g the acceleration of gravity, $s = c_s T + p/\rho + gz$ with c_s the specific heat at constant volume for the subsurface layer, and $h = c_p T + gz + Lq$ is moist static energy with c_p the specific heat of dry air at constant pressure and L the latent heat of condensation. Overbars denote time averages for periods much less than the seasonal time scale.

As shown in Fig. 1 the energy components in eq. (1) are: the land/ocean heat exchange $\overline{uh} = K(T_W - T_L)$ with K, T_W and T_L, the diffusion coefficient and the ocean and land surface temperatures, respectively; the meridional heat flux $\overline{vh}$; the vertical heat flux $\overline{wh}$; and the radiation heat flux R. Similar definitions are used in eq. (2) for the subsurface layer. The subsurface temperature is the same at the surface as bulk values. The storage and transport of kinetic energy have been neglected for the atmosphere (Oort, 1971). The storage and transport of latent heat of fusion (associated with ice and snow) have been neglected for the subsurface layer (Oort and Vonder Haar, 1976). The effects of salinity in the oceans have been neglected. The storage of latent heat Lq in the atmosphere cannot be neglected for the seasonal cycle (Oort, 1971). Rather than consider the moisture budget explicitly we simply prescribe the model relative humidity. Ice and snow albedo feedbacks are parameterized for both hemispheres. Empirically derived horizontal (meridional and zonal) heat flux parameterizations are used while the vertical dynamical heat flux is parameterized through dynamical adjustment processes using both the moist adiabatic lapse rate and the critical lapse rate for baroclinic adjustment (Wang et al., 1984). Note that the meridional heat flux is calculated based on averaged ocean and land temperature and is the same for both land and ocean sectors.

In the seasonal model, the solar radiation is based on Lacis and Hansen (1974), except that the frequency integration scheme described in Wang and Ryan (1983) is used to calculate the total solar flux. The parameterization includes the effects of absorption due to trace gases (CO_2, O_3, NO_2, O_2) and multiple scattering due to molecules (Rayleigh scattering) and cloud particles. The thermal radiation parameterization is based on the narrow band, correlated k-distribution method described in Wang and Ryan (1983). This method allows a rigorous treatment of coupled radiative processes of absorption and multiple scattering due to gases and particles in an inhomogeneous atmosphere. In the parameterization, twenty-seven narrow spectral intervals were used to account for the non-gray gaseous absorption of H_2O, CO_2, O_3, N_2O, CH_4, and CFCs and spectral properties of clouds, especially for high cirrus.

In order to simulate the current climate, we need to include the seasonal variation of ocean heat transport. However, information about ocean heat transport and its potential changes during climate changes are lacking. We use a simple approach. The value of ocean heat transport and storage for the present climate is derived from the model surface energy balance with (fixed) observed seasonal ocean surface temperature. During climate change experiments, the sum of the ocean heat transport and storage is assumed to remain the same as that of the present climate, while the ocean surface temperature is calculated. This approach has been used in GCMs (Hansen et al., 1984). Since ocean heat capacity is not explicitly treated, transient effects, which may cause warming delays ranging from decades to centuries, are not included (WMO, 1986; DOE, 1985b).

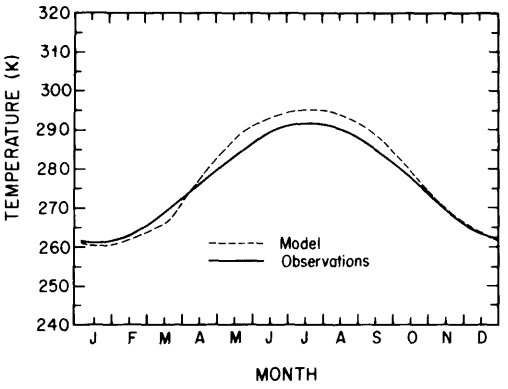

Fig. 2. Comparison of model calculated seasonal land surface temperature with observations for the northern zone 30–90° N.

Table 1. *Seasonal mean tropospheric lapse rate (°C km^{-1}) of northern zone (30–90° N). Both the model and observations correspond to averages between the surface and 100 mb. See Wang et al. (1984) for references of observations*

	Winter	Spring	Summer	Fall
model	3.9	4.5	5.2	4.9
observations	3.9	4.4	4.9	4.7

Fig. 2 shows the calculated land surface temperature of the present climate for 30–90° N. Both the phase and amplitude of the seasonal cycle are in good agreement with observations. Another good indicator of the model's ability to simulate the present climate is the model-calculated seasonal variation of tropospheric lapse rate, as shown in Table 1. The close agreement between model and observations indicates that the dynamical adjustment used in the model is capable of simulating the vertical temperature gradient, which is important in calculating the meridional and vertical sensible and latent heat transport (Wang et al., 1984; Gutowski et al., 1985).

2.2. *Photochemical-transport model*

The photochemical-transport model simulates the seasonal, latitudinal, and vertical distribution of atmospheric trace gases through chemical interactions among the gases and through dynamical transport. The global atmosphere is represented on a grid from south pole to north pole and from the ground to 60 km. The model resolution is approximately 10° of latitude in the horizontal and 3 km in the vertical.

The model contains over 40 chemical species which interact through over 100 chemical reactions. The chemical scheme employs the grouping technique to deal with chemicals having vastly different atmospheric lifetimes (cf. Ko et al., 1984). The kinetic reaction rates used in the calculation are those given by NASA/JPL (1985). The solar flux and absorption cross sections are from WMO (1986).

Dynamical transport within the model is caused by a zonal-mean circulation which varies seasonally and by eddy motions which serve to mix species along isentropic surfaces (see Ko et al., 1985a for description). The circulation employed is derived from prescribed diabatic heating rates based on values given by Murgatroyd and Singleton (1961). Concentrations of long-lived atmospheric species are integrated forward in time given by:

$$\frac{\partial \langle f \rangle}{\partial t} = -\langle v \rangle \frac{\partial \langle f \rangle}{\partial \phi} - \langle w \rangle \frac{\partial \langle f \rangle}{\partial p_e} + \frac{1}{\cos \phi} \frac{\partial}{\partial \phi} \left(K_{yy} \cos \phi \frac{\partial \langle f \rangle}{\partial \phi} \right) + \frac{\partial}{\partial p_e} \left(K_{zz} \frac{\partial \langle f \rangle}{\partial p_e} \right) + \langle P \rangle, \quad (3)$$

where f represents the mixing ratio of a trace atmospheric species; K_{yy} and K_{zz} are the horizontal and vertical eddy mixing coefficient respectively; and P_e is the equilibrium pressure coordinate (see Ko et al., 1985a). Chemical production and loss is represented in the term P. Angle brackets signify the zonal average of the quantity. K_{yy} is taken to be 3×10^9 cm^2 s^{-1} for all latitudes, heights, and seasons. Values of K_{zz} are 1×10^5 cm^2 s^{-1} in the troposphere, 1×10^3 cm^2 s^{-1} in the stratosphere, and 1×10^4 cm^2 s^{-1} above 45 km.

Long-lived species such as N_2O, CH_4, CH_3Cl, and CCl_4 have their sources in the troposphere and are dissociated in the middle and upper stratospheres. They are modeled by maintaining a fixed mixing ratio at the model lower boundary. The species, CFC-11 and CFC-12, are modeled

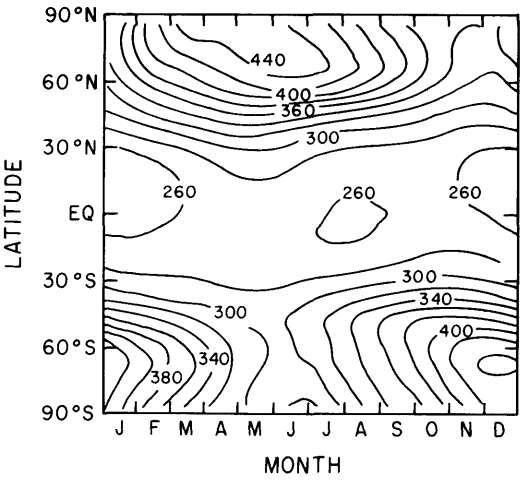

Fig. 3. Calculated O_3 column density (Dobson units) as a function of latitude and time for 1985.

by specifying the appropriate time dependent fluxes at the lower boundary.

The model calculated O_3 column abundance for 1985 is shown in Fig. 3. Compared to the corresponding observed O_3 column abundance (Bowman and Krueger, 1985), the model successfully simulates both the magnitude of the observed O_3 and its seasonal and latitudinal variation. The observed O_3 distribution illustrates the significance of dynamical transport: O_3 is primarily produced chemically in the tropics, but its maximum column abundance occurs near the poles. The calculated O_3 mixing ratios for January, April, July, and October are shown as a function of latitude and height in Fig. 4.

3. Results

The photochemical-transport model is used to calculate the changes in O_3 for the period 1960–2060 in response to increases in N_2O, CH_4, and CFCs. The surface concentrations of CH_4 and N_2O are assumed to increase at the rate of 1% per year and 0.25% per year, respectively. Time-dependent flux boundary conditions are used for CFC-11 and CFC-12 to simulate the release of the gases in the northern hemisphere. The release rates were assigned according to the values from the reporting companies (CMA, 1986) for the years 1960–1985. After 1985, the release rates are assumed to remain at the 1985 rates. The calculated changes in the column abundance and local concentration of O_3 between the years 1960 and 2060 are shown in Figs. 5 and 6, respectively.

In this open-loop calculation, the temperature and transport circulation are kept fixed at the initial prescribed values. Both are expected to change as the O_3 distribution is modified and the atmospheric burden of CO_2 increases. Previous calculations using 1-D (Luther et al., 1977) and 2-D (Haigh 1984) models showed that the stratospheric cooling caused by increase in CO_2 and trace gases would cause an increase in O_3. This O_3 increase will partially compensate for the model calculated O_3 decrease chemically associated with increases of trace gases. Therefore, ignoring this temperature feedback effect for O_3 led to an overestimation of the O_3 decrease in our model calculations. The effect of the circulation feedback on O_3 is highly uncertain. At the present stage of development, 2-D model predictions of how the wave-forcing might change with perturbed O_3 distributions and thermal structure have yet to be validated. If one assumes that the wave-driving is unchanged, the effect of a circulation change due to a change in radiative forcing should be small. The effect of circulation feedback will remain an active research topic in years to come.

The climate model is used to calculate the changes in temperature distribution caused by changes in these chemically-active gases and CO_2. For CO_2, we use observed values before 1985, while 0.55% per year is assumed to be the growth rate for the next few decades. The adopted surface mixing ratios for CO_2, N_2O, and CH_4 as well as the calculated surface mixing ratios for CFC-11 and CFC-12 for 1960, 1985 and 2060 are summarized in Table 2.

Two sets of calculations were performed. The first set calculates the changes in temperature taking into account only the changes in CO_2, N_2O, CH_4 and CFCs, the direct greenhouse effect, and ignores any changes in O_3. The effect of the O_3 change, as well as that of the other trace gases, is examined in the second set of calculations. First, we discuss the direct greenhouse effect. Because of the importance of cloud feedback, we have used two types of cloud treatment, the fixed cloud altitude (FCA) and the fixed cloud temperature (FCT) parameterization.

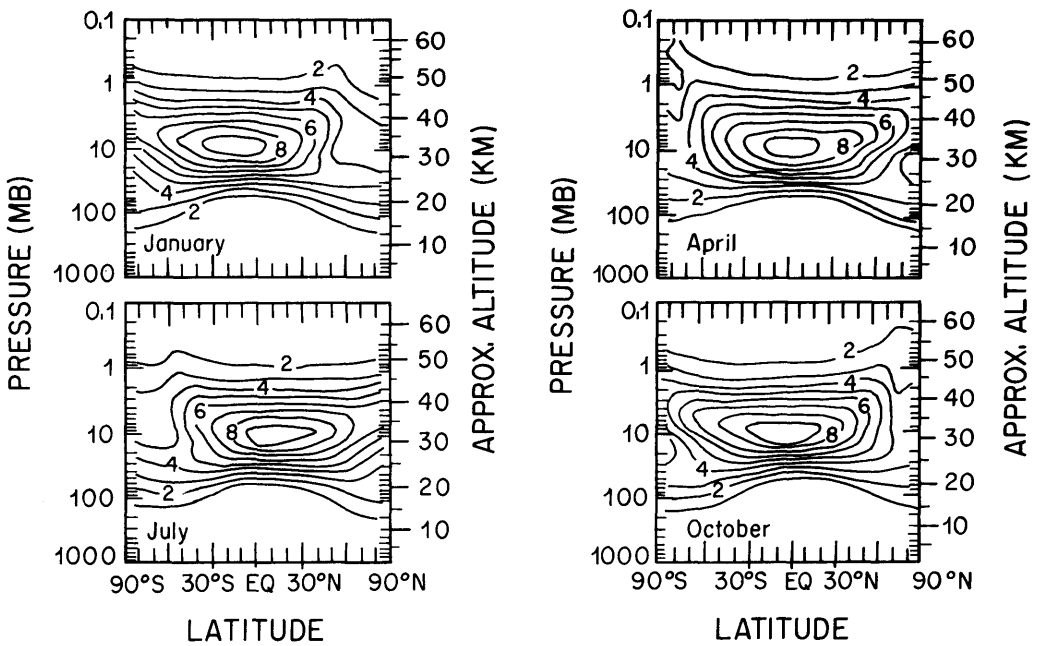

Fig. 4. Calculated cross sections of O_3 mixing ratio (ppmv) as a function of latitude and altitude for January, April, July, and October 1985.

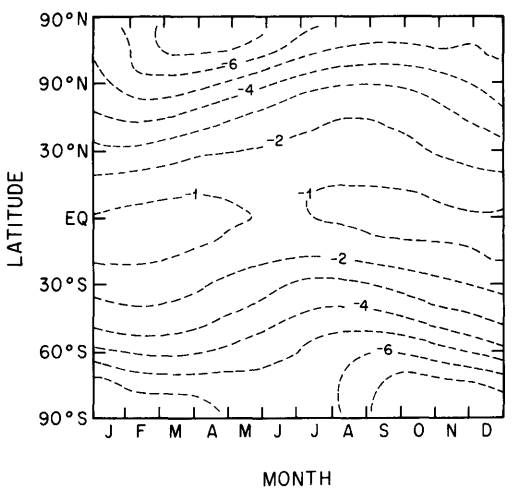

Fig. 5. Calculated percent change in the column abundance of O_3 between 1960 and 2060 for latitude and season. The emission of CFC after 1985 is assumed to continue at the 1985 rate. The surface concentrations of CH_4 and N_2O are assumed to increase at the rate of 1% per year and 0.25% per year respectively.

Compared to the FCA treatment, the FCT parameterization calculates a larger surface warming (Wang and Molnar, 1985) due to CO_2 doubling and is in closer agreement with GCM results (Hansen et al., 1984; DOE, 1985b). We use both parameterizations to illustrate the range of uncertainty associated with cloud treatment.

During the period 1960–1985, the increases of greenhouse gases are calculated to warm the annual mean and global mean surface temperature by 0.29°C for FCA (Table 3). A much larger surface warming 0.67°C is calculated for the FCT parameterization. Note that the observed increase in annual mean and global mean surface temperature for this period is about 0.3°C (Hansen and Lebedeff, 1987). The surface warming effect for the period 1985–2060 due to greenhouse gases alone is calculated to be 1.1 and 2.5°C for FCA and FCT, respectively.

Table 3 also gives a more detailed breakdown of the seasonal and latitudinal effects of an increase of atmospheric trace gases for both FCA and FCT treatments. In keeping with the annual

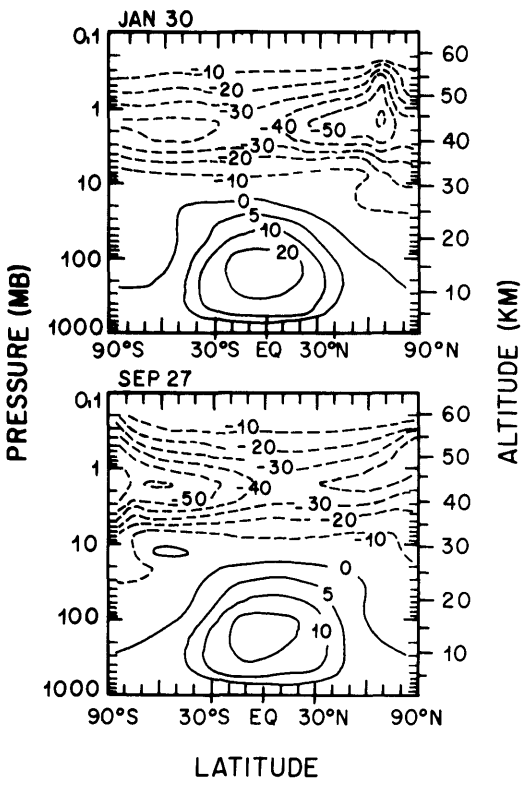

Fig. 6. Calculated percent change in the local concentration of O_3 between 1960 and 2060 for January and September. See Fig. 5 for description of scenario.

Table 2. *Global averaged surface mixing ratio used in this study*†

Trace gas species	Year 1960	1985	2060
CO_2 (ppmv)	317	347	525
N_2O (ppmv)	0.287	0.305	0.368
CH_4 (ppmv)	1.31	1.68	3.55
CFC-11 (ppbv)	0.116	0.227	0.714
CFC-12 (ppbv)	0.365	0.393	1.39

† Note that CO_2, N_2O, and CH_4 are prescribed and CFC-11 and CFC-12 are calculated from assumed surface emissions.

and global mean results, the FCT warming is consistently a factor of two greater than that for FCA for all latitude zones and seasons. As expected, both FCA and FCT cases show almost no seasonal variation within the tropical (30°S–30°N) zone. The extratropics, however, exhibit a more complex seasonal behavior reflecting the different responses of oceans and land. In the southern zone, where the ocean dominates, the zonal mean temperature increase tends to be larger during the summer than the winter. For the northern zone, where ocean and land fractions are nearly equal, the response of the land dominates resulting in a larger *winter* warming. For example, the 1985–2060 scenario, with an FCT treatment shows a northern zone warming of 2.9°C and 2.7°C for winter and summer, respectively. However, for the southern zone, the values for winter and summer are 2.3°C and 2.7°C. A closer look at the separate land and ocean responses reveals that both northern and southern oceans, as well as the southern land show the expected larger summer warming. In the northern zone over land, the larger *winter* warming is a direct result of the relatively large decreases in winter surface albedo derived from the increased snowmelt in both mid and high latitudes. In sharp contrast, the largest areas of snowcover in the southern zone are found in

Table 3. *Model calculated zonal mean and December–January–February (DJF) and June–July–August (JJA) mean surface warming (°C) due to increases of atmospheric trace gases shown in Table 2*†

Case		Period 1960–1985 FCA	1960–1985 FCT	1985–2060 FCA	1985–2060 FCT
30–90°N	DJF	0.38	0.79	1.4	2.9
	JJA	0.37	0.82	1.3	2.7
30°S–30°N	DJF	0.26	0.63	1.0	2.3
	JJA	0.26	0.63	1.0	2.3
30–90°S	DJF	0.29	0.68	1.2	2.7
	JJA	0.26	0.61	1.1	2.3
annual and global mean		0.29	0.67	1.1*	2.5

† The surface warming calculations consider only the direct greenhouse effect.

* The model calculates 1.2°C surface warming when both the direct greenhouse effect and the O_3 changes shown in Fig. 7 are considered.

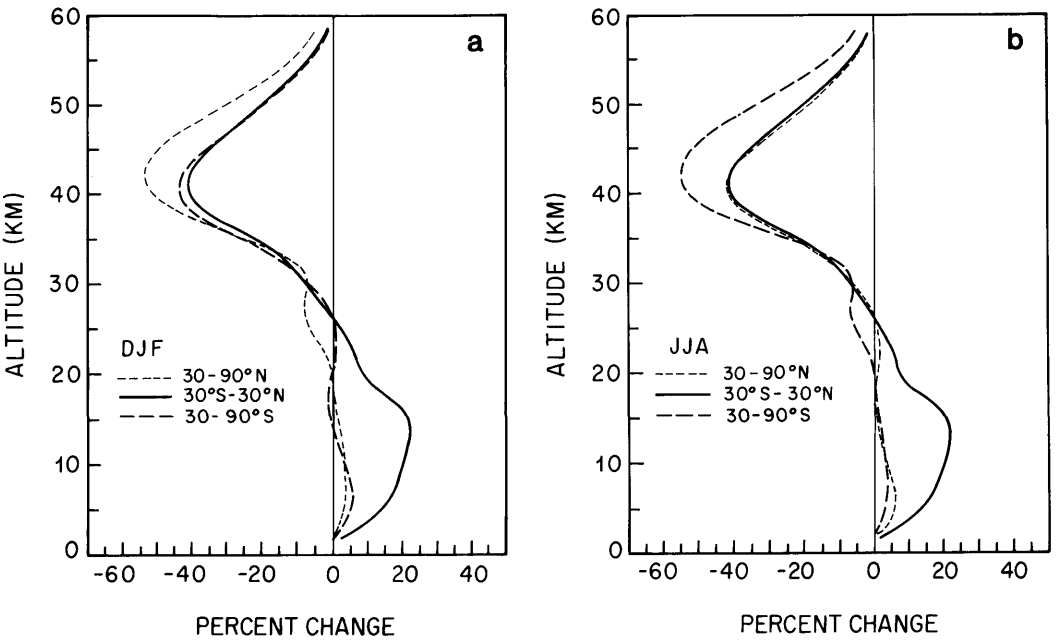

Fig. 7. Photochemical model calculated percent change in O_3 distribution between 1960 and 2060 for (a) December–January–February (DJF) and (b) June–July–August (JJA).

Antarctica, where almost no melting occurs at any time of year. It is thus the significantly greater land area and presence of snow at lower latitudes that allows the larger winter warming effect to dominate in the northern zone. This effect is also seen for the FCA 1960–1985 scenario.

Next, we used the climate model to calculate the effect of O_3 changes on surface temperature. Wang and Sze (1980) have shown that surface temperature is sensitive to changes in O_3 vertical distribution, especially in the lower stratosphere and upper troposphere. The photochemical-transport model calculated perturbations to atmospheric O_3 distributions between 1960 and 2060 are first averaged over the southern, northern, and tropical zones. The inputs to be used in the radiative calculation are shown in Fig. 7a for December–January–February (DJF) and in Fig. 7b for June–July–August (JJA). The results indicate that, for the southern and northern zones, there is relatively little change in O_3 throughout the troposphere, while for the tropical zone, the O_3 increases in the troposphere with a peak of about 25% around 13 km. In the stratosphere, all three zones show decreases of O_3 with maximum change occurring around 42 km.

The model-calculated change in DJF and JJA mean vertical distributions of temperature between 1985 and 2060 caused by changes in both O_3 and trace gases for FCA is shown in Fig. 8a for the tropics and Fig. 8b for the northern zone; the southern zone behaves much like the northern zone. The FCT results are very similar to the FCA case in the upper stratosphere. However, below about 15 km, the FCT gives a warming which is twice as large. In general, for all latitudinal zones, cooling occurs above 18 km and warming below. However, there are differences for different zones in the tropsphere as well as significant seasonal variations in the stratosphere of the high latitudinal zones. We will discuss these in more detail below. In addition, the results from a calculation that relate the effect of O_3 change on temperature are summarized in Table 4.

In the tropical zone, the maximum stratospheric cooling of about 12°C is calculated around 45 km, where the total cooling is caused mainly by the increased thermal emission due to

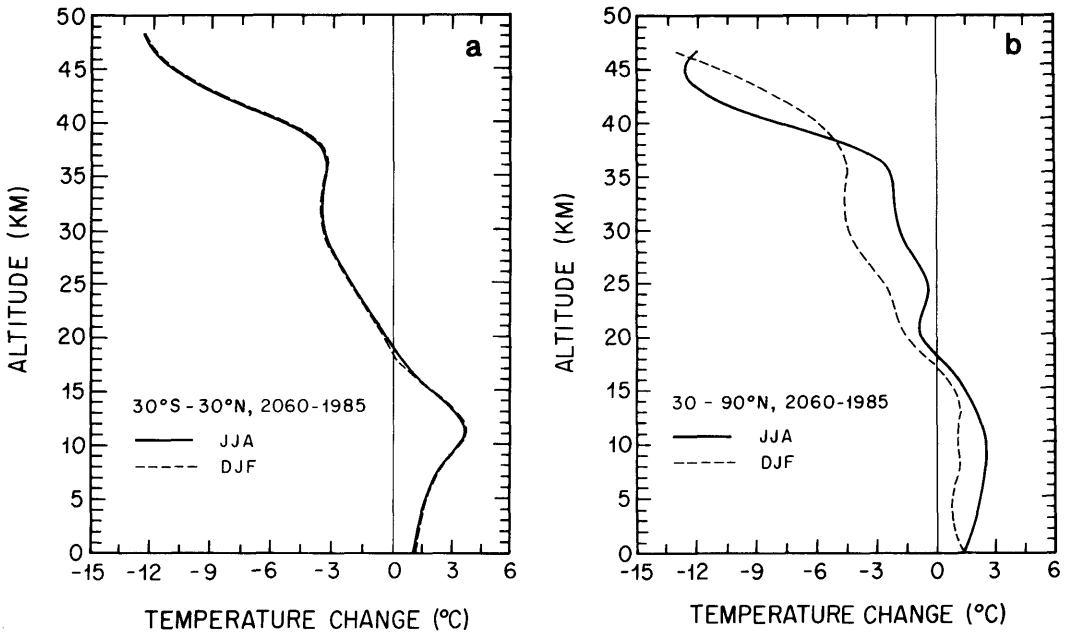

Fig. 8. Climate model calculated change in December–January–February (DJF) and June–July–August (JJA) vertical distribution of temperature between 1985 and 2060 for (a) 30°S–30°N and (b) 30–90°N. FCA parameterization is used.

CO_2 increases and to a lesser extent by decreased absorption of solar radiation due to O_3 depletion. However, around 42 km where the O_3 depletion peaks (see Fig. 7a), the cooling caused by O_3 decrease alone is calculated to be about 4.2°C (see Table 4), a substantial fraction of the total cooling shown in Fig. 8a. In the middle and lower stratosphere, the contribution of O_3 depletion to the total cooling is small because of the small and sometimes compensating changes in O_3 thermal cooling and solar heating. Consequently, the total cooling is again dominated by CO_2 increases. In the troposphere, the maximum warming of about 4°C calculated at 12 km is a factor of three larger than the surface warming. This feature, found also in GCM studies of the CO_2 climatic effect (cf. Chapter 4, DOE, 1985b), can be attributed to the moist adiabatic lapse rate used in the model. Note that, as expected, the seasonal variation is very small. The changes in O_3 distribution, shown in Fig. 7a, have a small effect on the tropospheric temperature (see Table 4). During the period 1985–2060, the O_3 changes alone warm the tropical tropopause region by 0.4°C while the surface warming effect is calculated to be about 0.06°C, contributing up to ~10% of the total effect.

Table 4. *Model-calculated zonal mean and December–January–February (DJF) and June–July–August (JJA) mean temperature change (°C) for the period 1985–2060 due to O_3 changes shown in Fig. 7; FCA parameterization is used*

Pressure (mb)	Altitude (km)	Tropical zone DJF	Tropical zone JJA	Northern zone DJF	Northern zone JJA
2.25	42	−4.2	−4.3	−2.2	−6.1
4	37	−0.44	−0.45	−0.53	−0.45
30	24	−0.06	−0.08	−0.31	0.04
150	14	0.38	0.39	0.09	0.08
surface	0	0.06	0.07	0.03	0.04

On the other hand, for the northern zone, much larger seasonal variations in both the troposphere and stratosphere are calculated. For example, the calculated middle and upper level warming in the troposphere in summer is about a factor of two larger than that in winter while the surface warmings are very close. Similar to the

tropical zone, the larger upper troposphere warming during summer can be attributed to the larger vertical dynamical heating. The larger cooling above 38 km during summer can be attributed mainly to the O_3 depletion and to a lesser extent to the larger thermal radiative cooling effects resulting from a warmer middle and upper stratosphere in summer than in winter.

We have further evaluated the relative contribution of the surface warming effect due to CH_4, N_2O, and CFCs to the total surface warming. Based on the scenario we used for the future increases of the trace gases, our model calculations indicate that by the middle of the next century, increases in CH_4, N_2O and CFCs may contribute 20%, 7%, and 10% respectively of the total surface warming. In other words, the combined effect of the other trace gases could augment the CO_2 surface warming by more than 60%. It should be noted that the results presented here are based on assumed emissions of CFCs at the 1985 rates. Recent control measures discussed at the Montreal meeting (UNEP, 1987) will limit the emissions of CFCs resulting in a smaller impact on greenhouse warming.

The increases in O_3 in the tropical troposphere lead to a small additional warming, which is in agreement with previous 1-D model results (Wang and Sze, 1980). For example, for FCA, the total surface warming is calculated to be 1.2°C for the period 1985–2060. The climatic effect of an O_3 change is small because of the small change in O_3 calculated in the lower stratosphere and upper troposphere. Recent analysis (Logan, 1985) suggests that tropospheric O_3 may be increasing at the rate of 1% per year. Such trends could be due to concurrent increases in concentrations of non-methane hydrocarbons and oxides of nitrogen in the troposphere, the effects of which are not included in our calculations. If this trend were to persist with the increase extending to the upper troposphere where the effect on climate is the largest, the impact of O_3 change on climate could be significantly larger.

4. Conclusions

We have used atmospheric models with seasonal cycles to study the effects on the distributions of atmospheric temperature and O_3 for the next few decades due to increasing atmospheric CO_2, CH_4, N_2O, and CFCs. The calculations indicate that the combined effect of the other trace gases could augment the CO_2 surface warming by more than 60%. The calculations suggest that by the middle of the next century the combined effect of the trace gases could warm the annual mean and global mean surface temperature by as much as 2.5°C with larger warming at high latitudes. In addition, much larger changes in atmospheric temperature are calculated. For example, the stratosphere could be cooled by about 12°C around 45 km and during summertime the middle to upper troposphere warmed by a factor of two to three larger than the surface warming. The effects of O_3 changes on the surface temperature, however, are small, primarily because of the small changes in O_3 calculated for the assumed scenarios of trace gases.

5. Acknowledgements

This research was supported by the Fluorocarbon Program Panel of the Chemical Manufacturers Association, the Climate Dynamics Program of the National Science Foundation (ATM-8805908), the Carbon Dioxide Research Division of the Department of Energy (DE-FG02-86ER60485) and the National Aeronautics and Space Administration (NASW-4080).

REFERENCES

Blake, D. R. and Rowland, F. S. 1988. Continuing worldwide increase in tropospheric methane, 1978 to 1987. *Science 239*, 1129–1131.

Bowman, K. P. and Krueger, A. J. 1985. A global climatology of total ozone from the Nimbus 7 Total Ozone Mapping Spectrometer. *J. Geophys. Res. 90*, D5, 7967–7976.

Chemical Manufacturers Association (CMA), 1986. Production, sales and calculated release of CFC-11 and CFC-12 through 1985. Chemical Manufacturers Association, 2501 M Street NW, Washington DC, October, 1986.

Cunnold, D. M., Prinn, R. G., Rasmussen, R. A., Simmonds, P. G., Alyea, F. N., Cardelino, C. A., Crawford, A. J., Fraser, P. J. and Rosen, R. D. 1986. Atmospheric lifetime and annual release estimates for $CFCl_3$ and CF_2Cl_2 from 5 years of ALE data. *J. Geophys. Res. 91*, 10797–10817.

DOE. 1985a. *Atmospheric carbon dioxide and global carbon cycle* (eds. M. C. MacCracken and F. M. Luther). Report *ER-0239*, US Department of Energy, Washington DC, 315 pp.

DOE. 1985b. *Projecting the climatic effects of increasing carbon dioxide* (eds. M. C. MacCracken and F. M. Luther). Report *ER-0237*, US Department of Energy, Washington DC, 381 pp.

Eckman, R. S., Haigh, J. D. and Pyle, J. A. 1987. An important uncertainty in coupled chlorine-carbon dioxide studies of atmospheric ozone modification. *Nature 329*, 616–619.

Gutowski, W. J., Wang, W.-C. and Stone, P. H. 1985. Effects of dynamic heat fluxes on model climate sensitivity: meridional sensible and latent heat fluxes. *J. Geophys. Res. 90*, 13081–13086.

Haigh, J. D. 1984. Radiative heating in the lower stratosphere and the distribution of ozone in a two-dimensional model. *Quart. J. R. Met. Soc. 110*, 167–185.

Haigh, J. D. and Pyle, J. A. 1982. Ozone perturbation experiments in a two-dimensional circulation model. *Quart. J. R. Met. Soc. 108*, 551–574.

Hansen, J., Lacis, A., Rind, D., Russell, G., Stone, P., Fung, I., Ruedy, R. and Lerner, J. 1984. Climate sensitivity: Analysis of feedback mechanisms. In: *Climate processes and climate sensitivity, Geophys. Monogr. Ser.*, vol. 29 (eds. J. E. Hansen and T. Takahashi). Washington, DC: AGU, 130–163.

Hansen, J. and Lebedeff, S. 1987. Global trends of measured surface air temperature. *J. Geophys. Res. 92*, 13345–13372.

Khalil, M. A. K. and Rasmussen, R. A. 1986. Interannual variability of atmospheric methane: possible effects of the El Niño-Southern Oscillation. *Science 232*, 56–58.

Khalil, M. A. K. and Rasmussen, R. A. 1989. Climate-induced feedbacks for the global cycles of methane and nitrous oxide. *Tellus*, in press.

Ko, M. K. W., Sze, N. D., Livshits, M., McElroy, M. B. and Pyle, J. A. 1984. The seasonal and latitudinal behavior of trace gases and O_3 as simulated by a two-dimensional model of the atmosphere. *J. Atmos. Sci. 41*, 2381–2408.

Ko, M. K. W., Tung, K. K., Weisenstein, D. K. and Sze, N. D. 1985a. A zonal-mean model of stratospheric tracer transport in isentropic coordinates: Numerical simulations for nitrous oxide and nitric acid. *J. Geophys. Res. 90*, 2313–2329.

Ko, M. K. W., Weisenstein, D. K., Sze, N. D. and Tung, K. K. 1985b. Simulation of O_3 distribution using a two-dimensional zonal-mean model in isentropic coordinate. In: *Atmospheric ozone* (eds. C. S. Zerofos and A. Ghazi). Dordrecht/Boston/Lancaster: D. Reidel Publ. Co., 19–23.

Lacis, A. and Hansen, J. 1974. A parameterization for the absorption of solar radiation in the earth's atmosphere. *J. Atmos. Sci. 31*, 118–133.

Logan, J. A. 1985. Tropospheric ozone: seasonal behaviour, trends and anthropogenic influence. *J. Geophys. Res. 90*, 10463–10482.

Luther, F., Wuebbles, D. J. and Chang, J. S. 1977. Temperature feedback in a stratospheric model. *J. Geophys. Res. 82*, 4935–4942.

Murgatroyd, R. J. and Singleton, F. 1961. Possible meridional circulation in the stratosphere and mesophere. *Quart. J. Roy. Meteor. Soc. 87*, 125–135.

NASA/JPL. 1985. Chemical Kinetics and Photochemical Data for Use in Stratospheric Modeling, Evaluation Number 7. NASA Panel for Data Evaluation, *JPL Publication, 85-37*, Jet Propulsion Laboratory, Pasadena, California.

Oort, A. H. 1971. The observed annual cycle in the meridional transport of atmospheric energy. *J. Atmos. Sci. 28*, 235–339.

Oort, A. G., Vonder Haar, T. H. 1976. On the observed annual cycle in the ocean-atmosphere heat balance over the northern hemisphere. *J. Phys. Oceanogr. 6*, 781–800.

Pearman, G. I., Etheridge, D., deSilva, F. and Fraser, P. 1986. Evidence of changing concentrations of atmospheric CO_2, N_2O and CH_4 from air bubbles in Antarctic ice. *Nature 320*, 248–250.

Ramanathan, V., Callis, L., Cess, R., Hansen, J., Isaksen, I., Kuhn, W., Luther, F., Mahlman, J., Reck, R. and Schlesinger, M. 1987. Climate-chemical interactions and effects of changing atmospheric trace gases. *Rev. Geophys. 25*, 1441–1482.

Rinsland, C. P., Levine, J. S. and Miles, T. 1985. Concentration of methane in the troposphere deduced from 1951 infrared solar spectra. *Nature 318*, 245–249.

Stone, P. H. 1984. Feedbacks between dynamical heat fluxes and temperature in the atmosphere. In: *Climate processes and climate sensitivity, Geophys., Monogr. Ser.*, vol. 29 (eds. J. Hansen and T. Takahashi). Washington, DC: AGU, 6–17.

UNEP. 1987. Montreal Protocol on substances that deplete the ozone layer. The United Nations Environmental Programme. Final Act. UN: New York.

Wang, W.-C. and Molnar, G. 1985. A model study of the greenhouse effects due to increasing atmospheric CH_4, N_2O, CF_2Cl_2 and $CFCl_3$. *J. Geophys. Res. 90*, 12971–12980.

Wang, W.-C., Molnar, G., Mitchell, T. P. and Stone, P. H. 1984. Effects of dynamical heat fluxes on model climate sensitivity. *J. Geophys. Res. 89*, 4699–4711.

Wang, W.-C. and Ryan, P. B. 1983. Overlapping effect of atmospheric H_2O, CO_2, and O_3 on the CO_2 radiative effect. *Tellus 35B*, 81–91.

Wang, W.-C. and Sze, N. D. 1980. Coupled effects of atmospheric N_2O and O_3 on the earth's climate. *Nature 286*, 589–590.

Wang, W.-C., Wuebbles, D., Washington, W. M., Isaacs, R. G. and Molnar, G. 1986. Trace gases and other potential perturbations to global climate. *Rev. Geophys. 24*, 110–140.

Washington, W. M. and Meehl, G. A. 1984. Seasonal cycle experiments on the climate sensitivity due to a doubling of CO_2 with an atmospheric general circulation model coupled to a simple mixed layer ocean model. *J. Geophys. Res. 89*, 9475–9503.

Wetherald, R. T. and Manabe, S. 1981. Influence of seasonal variation upon the sensitivity of a model climate. *J. Geophys. Res. 88*, 6600–6610.

WMO. 1986. *Atmospheric ozone 1985*. Global Ozone Research and Monitoring Project, Report No. 16, World Meteorological Organization, Geneva, 1095 pp.